Helium Solubility, Mobility, and Implantation Effects in Potassium Bromide*

R. C. Wayne and Walter Bauer
Sandia Laboratories, Livermore, California 94550
(Received 14 June 1972)

The solubility and mobility of He in single-crystal KBr has been determined using three methods: (a) permeation, (b) He release after soaking, and (c) ion implantation. Permeation experiments give values for the activation energies of diffusion and permeation of 0.34–0.39 and 0.63 eV, respectively, and a heat of solution of 0.29 eV. Measurements of gas release from crystals implanted with 10^{16} He^+ ions/cm^2 at 300 keV yield an activation energy for gas release of ~0.6 eV. The diffusion in the undamaged crystal is interpreted as due to interstitial motion of the He atom. A very low solubility, on the order of 10^{14} He atoms cm^{-3} atm^{-1}, was determined in the range of 100–200 °C, which is believed to be the first measured solubility of a rare gas in an alkali halide. Finally, it is shown that diffusion measurements such as those reported here for an undamaged crystal are insensitive to traps if typical concentrations and reasonable trap depths are used.

I. INTRODUCTION

Alkali halides provide a potentially simple system from which a basic understanding of rare-gas motion in solids can be obtained. In almost all previously published work,[1–4] rare-gas atoms were introduced into the lattice by energetic means, i.e., as nuclear-decay products, products of nuclear reactions, or as implanted positive ions.[4–17] As a result, significant lattice damage is present, which in general, greatly complicates the interpretation of the rare-gas mobility usually measured by gas release or isotopic distribution. In this work we have measured the mobility of helium in undamaged single-crystalline KBr by taking advantage of the small solubility of He in KBr, and have assessed the degree to which the results are representative of a perfect KBr lattice.

A description of the experiments in Sec. II is followed in Sec. III by the data and a comparison of the results obtained from the undamaged and implanted materials is given in Sec. IV. This paper reports the first known measurements of rare-gas solubility in alkali halides.

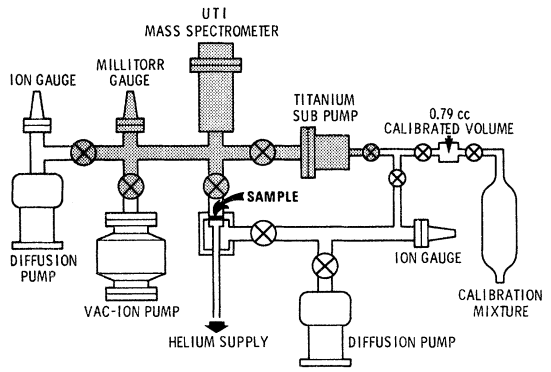

FIG. 1. Schematic of helium mass spectrometer used for all three types of measurements described in text. The main section consists of an all-metal bakeable vacuum system.

II. EXPERIMENTAL METHOD

The KBr crystals used were obtained from Harshaw and were found to contain the impurities shown in Table I. Analysis was made using both atomic absorption and emission spectroscopy.

Three techniques were used for measuring the He mobility in KBr. The first two, which allowed the use of undamaged crystals, employed introduction of the He either by soaking a crystal in a He atmosphere or by allowing the He to permeate through a thin disk. The third method involved introducing the He as 300-keV He^+ ions into crystals held at temperatures below 100 °K during irradiation.

A common aspect of all three experiments is that the He mobility was determined from gas release using a high-vacuum mass-spectrometer system such as is shown in Fig. 1. The He gas is continuously collected as it is released from a given sample. Calibration is accomplished both before and after an experimental run by admitting a known amount of hydrogen gas containing an accurately predetermined trace of helium. Using titanium sublimation pumps, all the reactive gases are re-

TABLE I. Chemical analysis of KBr.

Impurity	Mole fraction (ppm)	Valence	Number of vacancies (ppm)
Ca	<1	+2	2
Al	<3	+3	9
Si	<2	± 2	8[a]

[a]Si may contribute either positive- or negative-ion vacancies, thus possibly compensating for some of the negative-ion vacancies introduced by the Ca and Al.

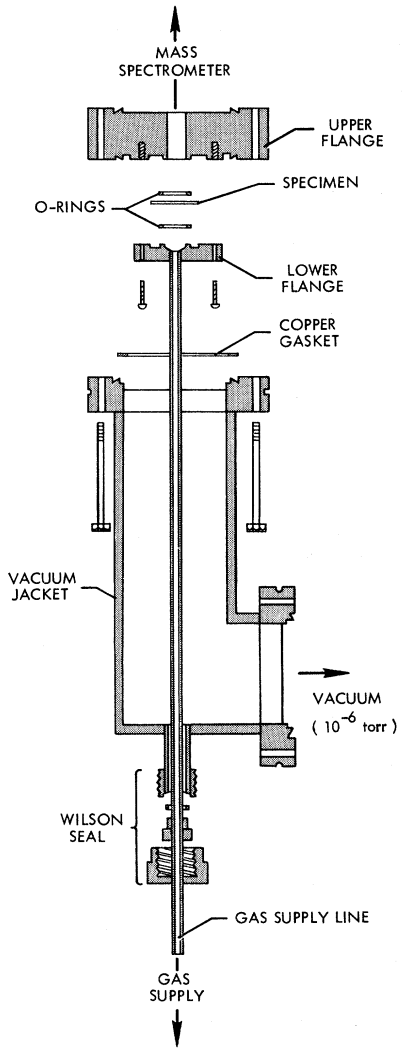

FIG. 2. Schematic of holder for disk permeation sample. The area between the two O rings is independently pumped to avoid leakage.

moved from the calibration mixture leaving only the He. An accuracy of approximately ±10% is achieved with a precision among measurements of 5%. During the experiment the background of reactive gases is kept below 10^{-7} Torr by the titanium sublimation pump.

Since the quantities of gas to be measured are often quite small (rates on the order of 10^7 atoms sec^{-1} in the permeation experiments) and may be released over a period of several hours, the background accumulation rate of He must be kept at a minimum. The background accumulation rate was held as low as 2×10^5 He atoms/sec by using an all-metal system (except for Viton seats in valves) which was baked at 200 °C for 48 h before use. In addition, a vacuum of 10^{-6} Torr was maintained behind all valves to the mass-spectrometer portion of the system since the residual helium in a poorer vacuum behind a well-seated valve could be readily detected. In all cases the background could be held to < 1% of the total signal. The major background contribution was attributed to outgassing from valve seats which were exposed to as much as 10^{-6} Torr He during the experiments.

Some helium can be trapped by the deposition of Ti on the walls of the Ti sublimation pump (~ one part in 10^4). Although this does not affect the accuracy of the measurement in progress it contributes to the background accumulation rate; thus whenever possible the titanium filament is kept off during the gas release. An active film of Ti is deposited before the experiment and is sufficient to continue pumping reactive gases under normal experimental conditions for at least a day. Finally, to avoid pumping by ionization processes, no vacuum gauges are left operating during the measurements. This pumping is a measurable effect in such high-sensitivity experiments.

Of the three approaches employed here, *soaking* the crystal in He with subsequent release required the least system sensitivity. The advantage of this technique lies in the ability it affords to examine substances with very low permeability and solubility over a wide temperature range. A crystal of convenient geometry is soaked at a known pressure of He (usually 400 Torr in these experiments) and a given temperature for a time sufficient to assure that equilibrium conditions have been reached. Transfer of the crystal to the mass-spectrometer chamber (and associated temperature excursion if any) takes a few minutes. During this time up to a few percent of the helium may be lost. In addition one must consider possible spurious effects due to helium which is adsorbed on the surfaces of the sample.

In the second method, *permeation*, helium is allowed to diffuse through a KBr crystal by establishing a concentration gradient across the sample. A 0.1-cm-thick disk is mounted as shown in Fig. 2 with vacuum on both sides.[18] In addition, a vacuum of better than 10^{-6} Torr is maintained between the Viton O rings in order to prevent the He which permeates through the O-ring seal on the back of the sample from permeating through the O-ring seal to the mass-spectrometer portion. The experimental procedure involves establishing the background rate, and then admitting a known pressure of He behind the sample. After an induction period, the rate at which He permeates through the crystal reaches an equilibrium value (as shown in Fig. 3). If the permeability K is sufficient to be measured, then both the diffusivity D and solubility S can be independently obtained ($K = DS$). The value of D can then be obtained either from the induction portion of the permeation curve or from the decay

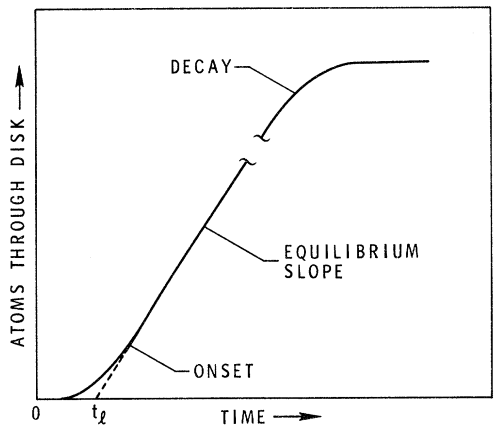

FIG. 3. Schematic plot of typical pressure time dependence on the downstream side of sample during permeation experiment. There are three distinct regions: (i) the onset when a helium pressure is first applied to the upstream side, (ii) equilibrium when the concentration gradient in the sample is constant in time, and (iii) the decay when the helium is removed from the upstream side of the sample.

of the gas after the He is removed from behind the crystal. Unfortunately, the temperature over which permeation can be measured is limited to the range from 100 to 240 °C by background considerations at the low-temperature end and the Viton O rings used to seal the sample at the high-temperature end.

Finally, 300-keV He^+ ions were implanted in the crystal to obtain an estimate for the role of implantation damage. The implantation technique affords the opportunity of measuring much lower diffusion coefficients (than via bulk-diffusion techniques) due to the small distances involved. The reason for this is that the range of the 300-keV He^+ ions in KBr is ~1 μm, and for a given value of D the time for the measurement scales as the square of the range. During implantation, the temperature of the crystal was held below 100 °K with the He subsequently released during isothermal anneals around room temperature. Experiments were performed on two types of samples: The first were on virgin crystals, the second on a crystal which was repeatedly implanted and subsequently annealed to 275 °C. This temperature was high enough to release the He but not necessarily to anneal all the radiation damage. The latter experiments were done to assess the cumulative nature of any lattice damage which may remain after the He is released from the sample.

III. RESULTS AND DISCUSSION

A. Helium Release after Soaking KBr in Helium Atmosphere

In principle both the diffusion coefficient D and solubility S can be obtained from the soaking method, D from the rate at which He is absorbed by or is released from the crystal and S from the total number of atoms present under equilibrium conditions. The sample geometry used in these experiments was that of a cleaved right-rectangular solid of dimensions $1.70\times1.77\times0.39$ cm. Values of D were obtained at a given temperature from a solution of Fick's law by fitting the fractional He release F to the expression[19]

$$F=1-\left(\frac{8}{\pi^2}\right)^3\prod_{\nu=1}^{3}\sum_{n=0}^{\infty}\frac{1}{(2n+1)^2}\exp\left[-\left(\frac{(2n+1)\pi}{h_\nu}\right)^2 Dt\right], \quad (1)$$

where the h_ν are the crystal dimensions, t is the time from the start of release, and D is assumed constant and isotropic throughout the crystal.

Helium adsorption on the surface may play a significant role in the gas release. In Fig. 4 we have plotted the total-helium-gas-release data at 28 °C after soaking. As can be seen, the data do not fit the simple diffusion-theory solution given in Eq. (1). The difference between the data and theory can be described by a single exponential which has effectively reached its asymptotic value after ~8 $\times10^3$ sec. We attribute this contribution to the outgassing of helium adsorbed on the surface of the crystal. To evaluate this effect the amount of He adsorbed on samples was determined by etching the surface with water after soaking and before measuring the gas release. The water-etched crystals had an effective solubility 20–30% lower than equivalent but not etched crystals. From this we conclude that surface sorption does play a role, at least at 300 °K, and suggest that 10^{-3} and 10^{-4}

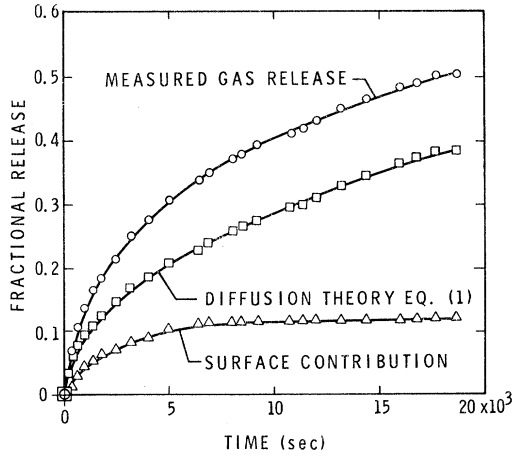

FIG. 4. He release during isothermal anneal after soaking. The data are the sum of two components: The first contribution is due to normal bulk diffusion following Eq. (1) of text; the second contribution is attributed to He desorbed from the surface and follows a simple exponential.

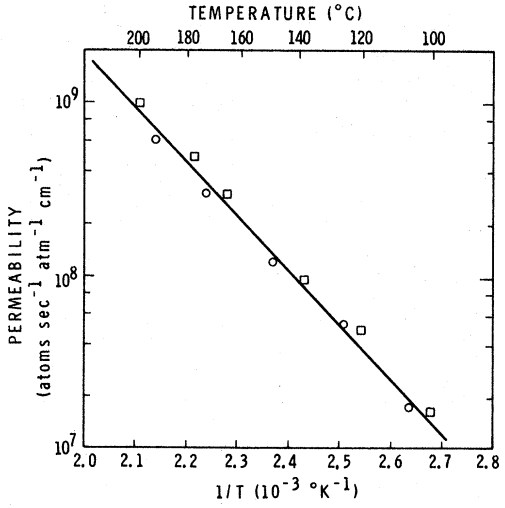

FIG. 5. Plot of permeability vs $1/T$, where T is the temperature at which the equilibrium permeation rate was measured. An activation energy of 0.63 eV is obtained from the slope of the straight line. Data from two samples are shown to indicate consistency.

monolayer of He is shallowly trapped. At temperatures of 100 °C and above, this contribution becomes undetectable, probably due to the greater bulk solubility. In all cases, the values of D obtained from the soaking data represented a fit of the data to a calculated $F(t)$ function over a wide range of time, usually 10^4 to 3×10^4 sec.

Owing to the low bulk solubility of He in the crystal, the possibility of He being trapped exclusively or partially at defect sites must be considered. A chemical analysis of one of the crystals (given in Table I) shows the presence of impurities sufficient to give rise to a 10^{-5} concentration of negative-ion vacancies. In the temperature range employed in these experiments, thermal vacancies can be neglected. The effect of these impurity-induced vacancies will be discussed.

B. He Permeation through KBr

The permeability K of He through KBr can be obtained directly from the equilibrium permeation rate of helium R through a crystal of area A, thickness h, and a fixed pressure differential P:

$$K = Rh/AP \ . \tag{2}$$

The permeability data obtained using Eq. (2) are plotted in Fig. 5. The data fit a straight line representing an activation energy of permeation of 0.63 eV. The value for D is determined from either the onset portion of the permeation curve (see Fig. 3) or from the decay portion occurring after all He is removed from behind the sample. During the onset portion the He accumulates following

$$C(t) = \frac{DSAPt}{h} + \frac{2SAPh}{\pi^2}\sum_{n=1}^{\infty}\frac{(-1)^n}{n^2} \times\left[1-\exp\left(\frac{-n^2\pi^2 Dt}{h^2}\right)\right] , \tag{3}$$

and during the decay portion

$$C(t) = -\frac{2SAPh}{\pi^2}\sum_{n=1}^{\infty}\frac{(-1)^n}{n^2}\left[1-\exp\left(\frac{-n^2\pi^2 Dt}{h^2}\right)\right] , \tag{4}$$

where $C(t)$ is the concentration of He in atom Torr. An expression directly in terms of D can be obtained from Eq. (4) for long times as

$$D = \frac{h^2\{\ln[C'(t_1)/C'(t_2)]\}}{\pi^2(t_2-t_1)} \ , \tag{5}$$

where $C'(t)$ is the time derivative of Eq. (4). D can be obtained from the uptake portion of the permeation curve by extrapolating the steady-state (straight line) segment of $C(t)$ back to the $C=0$ axis, as shown by the dotted line in Fig. 3. This intersection defines a lag time t_l such that

$$t_l = h^2/6D \ . \tag{6}$$

An activation energy of diffusion is then derived from a plot of log D vs T^{-1} as shown in Fig. 6. From the values of K and D (shown in Figs. 5 and 6, respectively) and the relation $K=DS$, the solubility S was then determined. The values are plotted in Fig. 7. Again, there is good fit to a straight line representing an enthalpy of solution of 0.29 eV. A summary of the results is given in Table II.

In the permeation experiments the surface contribution can be neglected since it affects only ~10^{-3}

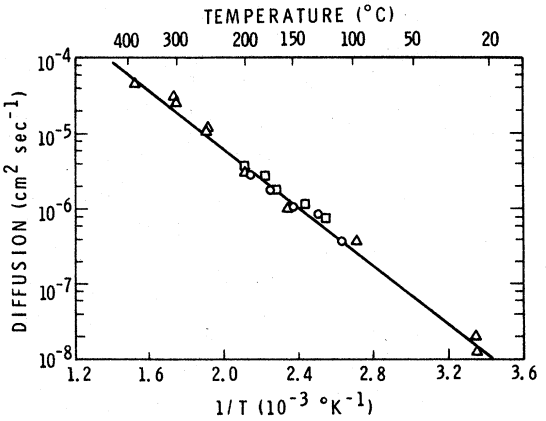

FIG. 6. Plot of the diffusion coefficient D vs $1/T$. D was determined from Eqs. (5) and (6) of the text during the uptake and decay portions of the permeation measurements except in the case of the triangles, which represent values of D obtained from the soaking technique using Eq. (1). An activation energy of 0.39 eV is found from the slope of the straight line. Data from two samples are shown to indicate consistency.

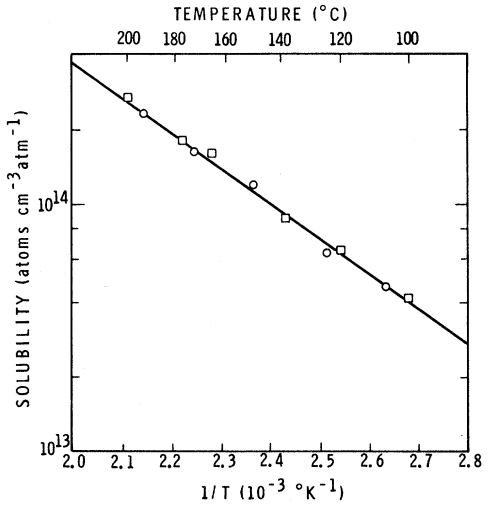

FIG. 7. Plot of the solubility vs $1/T$. At each temperature T the solubility was determined from $K=SD$ using the data of Figs. 5 and 6. An enthalpy of solution of 0.29 eV is found from the slope of the straight line. Data from two samples are shown to indicate consistency.

atom fraction of the atoms which permeate through the crystal. This is in contrast to the situation observed in soaking where 10^{-3} to 10^{-4} of the surface sites appear to be occupied, representing 0.1 to 0.01 fraction of the helium contained in the bulk.

C. Effect of Trapping

In order to interpret the measurements, the importance of trapping of He by defects (such as vacancies) must be determined. An estimate of the contribution from traps can be made using the model of Sosin and Bauer.[20] So that the calculated curves could be related to the measured gas release, the equations in Ref. 20 were modified for the case of a right-rectangular solid (see Appendix) to conform to the sample shape used in the soaking experiments. From the results of the calculations, several conclusions could be drawn. First, the He-release curve predicted from the model is of exactly the same functional form as Eq. (1) regardless of the concentration or depth of the traps for the time scales pertinent to these experiments. The reason for this is that the trap depth must be greater than 1 eV, an unrealistically large value, in order to prevent a dynamic equilibrium between the trapped and untrapped species from being reached in a few seconds. These experiments are not sensitive to such a time scale. Thus an effective value of D could be obtained as was done in the soaking experiments for reasonably realistic trap depth and concentrations. Second, if E_D represents the activation energy for He diffusion in the bulk of the crystal and $E_T = E_D + \Delta E$ represents the trap depth, an estimate of the maximum value of ΔE can be made. In Fig. 8 are shown six curves calculated from the equations in the Appendix following $D_0 = 5.2\times10^{-2}$ cm^2/sec; a fractional concentration of traps $C_T = 10^{-5}$ and the values of E_D and ΔE are given in Fig. 8. The theoretical curves were fitted to the data at 400 °K. Clearly, for the realistic choice of $C_T = 10^{-5}$, ΔE can be no greater than 0.25 to 0.30 eV and still achieve a reasonable fit to the data. Using an upper limit of $C_T = 10^{-4}$ yields a maximum depth of $\Delta E = 0.22$ eV. This demonstrates that trapping processes with $C_T = 10^{-5}$ and $\Delta E \sim 0.30$ eV may exist but are not discernible by gas-release experiments. That is, if the data follow a straight line on an Arrhenius plot such as Fig. 8, one cannot interpret that evidence as proving that no trapping exists at an atomistic level. However, if that level of trapping exists it is inconsequential to the bulk-diffusion process.

Finally, suppose the traps were to completely dominate the gas release. In order to fit the experimental data the trap depth would have to be ~0.39 eV. Again using a value of $C_T = 10^{-5}$ an upper limit on the activation energy for diffusion of He in the bulk can be calculated. This upper limit is ~0.04 eV, a clearly unrealistically low value. For this reason we do not believe that traps are dominant.

The measured values of E_D can also be compared to the theoretical work of Wilson[21] and of Norgett and Lidiard.[22] Wilson obtains a value of ~0.2 eV for interstitial motion of He in KBr. Norgett and Lidiard obtain a range of values from 0.15 to 0.26 eV for interstitial motion of Ar in KBr. In addition they indicate that this value is a lower limit on E_D. Although the measured activation energies are approximately twice these calculated values we consider our results to be consistent with interstitial diffusion.

D. Helium Implantation and Outgassing

An inevitable side effect of implantation is the creation of lattice defects in the vicinity of the helium and in the region between the implanted layer and the surface of the crystal. Figure 9 shows the cumulative effect of the damage remaining after 275 °C anneal on the release of implanted helium. From the data shown in Fig. 9 it is clear that ex-

TABLE II. Results of soaking and permeation experiments.

	Soaking	Permeation
K_0 (atom sec^{-1} atm cm^{-1})	•••	4.49×10^{15}
E_k	•••	0.63 eV
S_0 (atom cm^{-3} atm^{-1})	•••	2.88×10^{17}
E_s	•••	0.29 eV
D_0 (cm^2 sec^{-1})	5.2×10^{-2}	1.42×10^{-2}
E_D	0.39 eV	0.32 eV

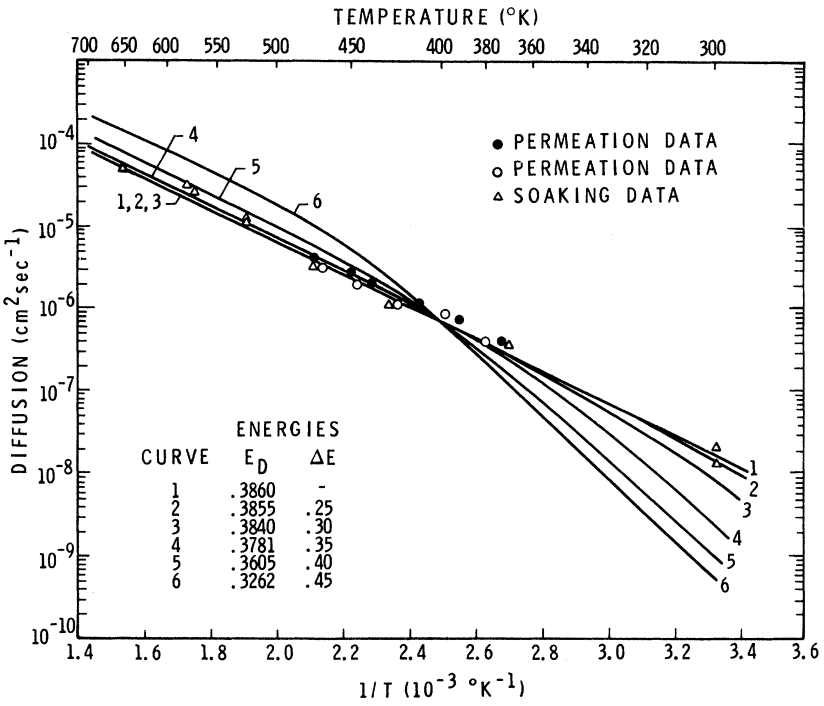

FIG. 8. Plot of diffusion coefficients vs $1/T$. In addition to the measured data, calculational results are included using the model described in the Appendix with a range of trap depths ΔE and activation energy of diffusion E_D for a trap concentration of 10^{-5}.

periments designed to obtain an activation energy representative of the same damage state require use of a new undamaged crystal for each implantation. A series of 10^{16}-atom/cm^2 implantations were made at ~100 °K with subsequent isothermal anneals at temperatures of 20, 30, 50, and 72 °C. The He release follows the same functional form at all temperatures, allowing the calculation of an activation energy. Figure 10 is an Arrhenius plot of the relative-diffusion coefficients for 10^{16}-atom/cm^2-dose implants and yields a diffusion activation energy of 0.58 eV. Similar data for 10^{15} atom/cm^2 yield a value of ~0.5 eV. This activation energy for diffusion (0.5 to 0.58 eV) is significantly greater than that in the undamaged crystal (0.34 to 0.39 eV). As a result, it is suggested that the rate-determining step in the He release after implantation involves traps created by the implantation.

Information on the kinetics can be gained from

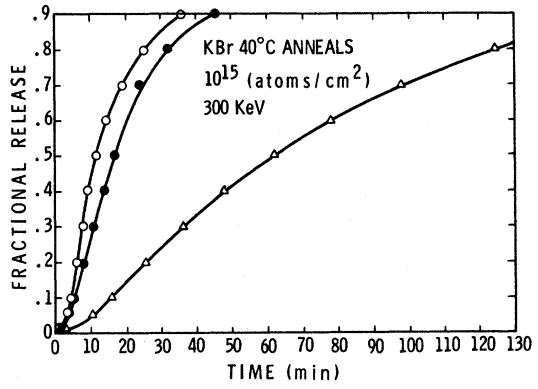

FIG. 9. Fractional He release is shown as a function of annealing time at 40 °C in all cases. The open circles show the He release for a virgin crystal implanted to 10^{15} He$^+$ ions/cm^2, and the closed circles show the He release for the same crystal following a 275 °C anneal for 10 min and a reimplantation to 10^{15} He$^+$ ions/cm^2. The triangles show the He release from the same crystal after another 275 °C anneal, an 8×10^{15}-He$^+$-ion/cm^2 implantation, a subsequent 275 °C anneal, and finally a 10^{15}-He$^+$-ion implantation.

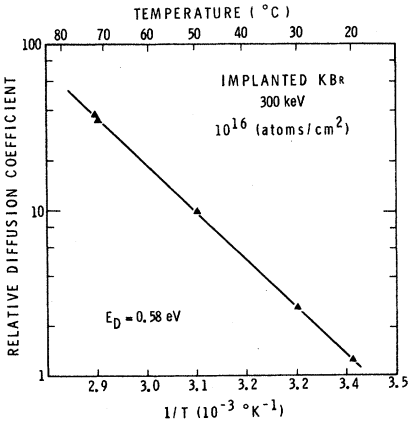

FIG. 10. Arrhenius plot of relative diffusion coefficient vs $1/T$. An activation energy of diffusion of 0.58 eV is determined from the slope.

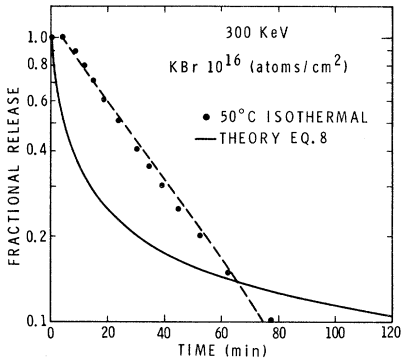

FIG. 11. Fractional helium release at 50 °C after implantation at 300 keV. The data fit an exponential in Eq. (7) of text rather than a function as in Eq. (8) of text. The latter is a representative of a diffusion process.

the shape of the helium-release curves. An example of such a curve is given in Fig. 11. In addition to the data plotted on a semilog plot a theoretical curve following simple diffusion theory is shown. In Fig. 11 it can be seen that the gas release follows a first-order rate equation,

$$F = 1 - e^{-t/\tau} , \tag{7}$$

reasonably well (dashed line). The parameter τ can be expected to be relatively independent of the range R and should depend primarily on the trap depth governing the process. Simple diffusion theory with no trapping requires that the release follow

$$F = 1 - \mathrm{erf}(R/4(Dt)^{1/2}) \tag{8}$$

shown by a solid line in Fig. 11. As is readily apparent from Fig. 11, the data do not fit the solid curve. This is thought to be additional evidence that the helium release is governed by a rate-determining step within the implanted layer, rather than by a simple concentration gradient.

Finally, it should be noted that He complexes within the implanted layer probably play a role since the local He concentration is ~10^{-2} atom fraction, far in excess of the solubility shown in Fig. 7. Nucleation into small bubbles or simply multiple He-atom defects may be important.

IV. SUMMARY AND CONCLUSIONS

It has been shown that defects or clustering due to energetic forms of introduction such as implantation of He affect both the measured diffusion activation energy and release kinetics of He in KBr. Permeation experiments on the undamaged material give an activation energy for diffusion of ~0.39 eV whereas 0.58 eV is obtained for the implanted samples. It is proposed that the He moves interstitially in the undamaged KBr crystal and that trapping dominates in the case of the implanted material; however, it is still possible that the He atoms are encountering shallow traps in the undamaged case as well. It has been established that these traps can be no more than 0.3 eV deep. Finally, it has been demonstrated that helium has a measurable solubility in at least one alkali halide, a fact which has not been previously reported.

ACKNOWLEDGMENTS

We wish to acknowledge the invaluable aid of W. L. Chrisman and D. H. Morse in performing these experiments. In addition we benefited from many fruitful discussions with W. D. Wilson. Finally we wish to thank G. W. Anderson, W. D. Wilson, and J. E. Shelby for critical reading of the manuscript. Preliminary measurements in this program were made with the equipment and cooperation of J. B. Holt.

APPENDIX

The equations used to evaluate the effect of trapping on the He diffusion are as follows[20]:

$$\frac{\partial i}{\partial t} = D\nabla^2 i - \lambda i + \mu s , \tag{A1}$$

$$\frac{\partial s}{\partial t} = \lambda i - \mu s . \tag{A2}$$

Here i and s are the concentrations of He in the bulk (perhaps interstitial) sites and in traps (perhaps substitutional sites), respectively; λ and μ are the rate constants for motion out of the respective sites and are defined as

$$\lambda = 24 C_T \nu e^{-E_i/kT} , \tag{A3}$$

$$\mu = 24\nu e^{-E_s/kT} . \tag{A4}$$

The parameter C_T is the concentration of traps relative to the bulk sites, ν is the attempt frequency, and E_i and E_s the respective depths of the bulk and trap potential wells containing He atoms. The number 24 represents the total number of interstitial sites to which a He atom can go from a trap assumed to be a vacancy.

These equations were solved explicitly for a cylindrical geometry by Sosin and Bauer. In that case the solutions can be separated into $i(r,t)$ and $s(r,t)$ contributions where r is the radial coordinate. For the rectangular solid, this separation into trapping and bulk contributions is not possible and the solution for the amount of He retained must be written

$$\frac{C_{xyz}(t)}{C_0} = \left(\frac{8}{\pi^2}\right)^3 \left(\frac{1}{1+f}\right)^3 \prod_{j=1}^{3} \sum_{n=0}^{\infty} \left(\frac{1}{2n+1}\right)^2 (T_{ijn} + T_{sjn}) . \tag{A5}$$

Here f is defined as the initial ratio of substitutional to interstitial He atoms, and following the nota-

tion of Ref. 20,

$$T_{ijn}=\{[P^{+}_{nj}+\mu(1+f)]\,e^{P^{+}_{nj}t}-[P^{-}_{nj}+\mu(1+f)]\,e^{P^{-}_{nj}t}\}\times(P^{+}_{nj}-P^{-}_{nj})^{-1},$$

$$T_{sjn}=\frac{\lambda[P^{+}_{nj}+\mu(1+f)]\,e^{P^{+}_{nj}t}}{(P^{+}_{nj}-P^{-}_{nj})(P^{+}_{nj}+\mu)}-\frac{\lambda[P^{-}_{nj}+\mu(1+f)]\,e^{P^{-}_{nj}t}}{(P^{+}_{nj}-P^{-}_{nj})(P^{-}_{nj}+\mu)},$$

where the P_{nj} values are the roots of the equation

$$P^{2}_{nj}+P_{nj}(\lambda+\mu-K_{nj})-\mu K_{nj}=0$$

and

$$K_{nj}=-D[(2n+1)\,\pi/h_j]^2,$$

with the h_j being the lengths of the respective sides.

*Work supported by the U. S. Atomic Energy Commission, Contract No. AT-(29-1)-789.

[1]T. S. Elleman, C. H. Fox, and L. D. Mears, J. Nucl. Mater. 30, 89 (1968).
[2]W. A. Stark, Bull. Am. Phys. Soc. 17, 83 (1972).
[3]R. C. Wayne and W. Bauer, Bull. Am. Phys. Soc. 16, 341 (1971).
[4]R. C. Wayne and W. Bauer, Bull. Am. Phys. Soc. 17, 287 (1972).
[5]A. Ong and T. S. Elleman, J. Nucl. Mater. 42, 191 (1972).
[6]F. W. Felix, Proc. Brit. Ceram. Soc. 9, 273 (1967).
[7]S. Kalbitzer, Z. Naturforsch. 17a, 1071 (1962).
[8]H. P. Mundt and A. K. H. Richter, Z. Naturforsch. 20a, 267 (1965).
[9]T. S. Elleman, L. D. Mears, and R. P. Christman, J. Am. Ceram. Soc. 51, 560 (1968).
[10]P. Schmeling, J. Phys. Chem. Solids 28, 1185 (1967).
[11]F. W. Felix, Phys. Status Solidi 27, 529 (1968).
[12]W. Bannasch and P. Schmeling, J. Phys. Chem. Solids 26, 1999 (1965).
[13]P. Schmeling, Phys. Status Solidi 11, 175 (1965).
[14]Hj. Matzke and J. L. Whitton, Can. J. Phys. 44, 995 (1966).
[15]Hj. Matzke and C. Jech, J. Phys. Chem. Solids 31, 753 (1970).
[16]P. P. Pronko and R. Kelly, Appl. Phys. Letters 18, 335 (1971).
[17]A. Sy Ong and T. S. Elleman, J. Nucl. Mater. 42, 191 (1972).
[18]This means of performing permeation experiments was first devised by J. E. Shelby.
[19]Much of the basic analysis can be found in W. Jost, *Diffusion in Solids, Liquids, and Gases* (Academic, New York, 1960), Chap. 1.
[20]A. Sosin and W. Bauer, Phys. Rev. 147, 478 (1966).
[21]W. D. Wilson (private communication).
[22]M. J. Norgett and A. B. Lidiard, Phil. Mag. 18, 1193 (1968).

PHYSICAL REVIEW B VOLUME 6, NUMBER 10 15 NOVEMBER 1972

Dipole Relaxation, Aggregation, and X-Ray Effects in KCl Doped with Eu^{++}, Yb^{++}, or Sm^{++} †

S. Unger and M. M. Perlman
Department of Physics, Collège militaire royal de Saint-Jean, Saint-Jean, Québec, Canada
(Received 26 June 1972)

The behavior of impurity-vacancy (I-V) dipoles has been studied in KCl single crystals doped with Eu^{++}, Yb^{++}, or Sm^{++}, using the ionic-thermocurrents technique. The activation energies and frequency factors for dipole relaxation have been determined. The aggregation of these dipoles in KCl:Eu^{++} follows third-order kinetics in the temperature range 295–323 °K, and their decay rate is comparable to that of KCl:Sr^{++}. The activation energy and frequency factor for the formation of trimers have also been determined. It has proved possible to destroy these rare-earth I-V dipolar systems by irradiation with x rays, and to recover them on subsequent heating or irradiation with a Xe-Hg lamp. This process is postulated to take place through charge conversion of the I-V dipole constituents.

I. INTRODUCTION

In recent years, alkali-halide crystals doped with various doubly valent impurity cations have been studied[1–4] to determine the parameters associated with cation-vacancy motion, when the vacancy is either free, or associated with an impurity in an impurity-vacancy (I-V) dipole.

In the first instance, obtainable at temperatures above 300 °C,[5] the appropriate activation energy and frequency factor are determined from dc ionic-conductivity measurements.[2] At lower temperatures, where significant pairing takes place, the methods of dielectric absorption[6] and ionic thermocurrents (ITC)[7] may be employed to determine the parameters associated with dipole rotation and diffusion. It is the latter technique that has been used here.

In much of the previous work on the aggregation of I-V dipoles, the results have been analyzed